Highly Reliable Blue Phosphor-Sensitized Fluorescent Tandem Organic Light-Emitting Diode Utilizing Spontaneous Orientation Polarization in Electron-Transport Layer

Hiromitsu Kido, Takeyoshi Watabe, Toshiki Sasaki, Hiromi Nowatari, Keito Fukuda, Nobuharu Ohsawa, and Shunpei Yamazaki

Semiconductor Energy Laboratory Co., Ltd., Kanagawa, Japan

Abstract

The recombination region in a light-emitting layer in a blue phosphorescent organic light-emitting diode (OLED) was controlled through spontaneous orientation polarization in an electron-transport layer. We developed a blue phosphor-sensitized OLED using a fluorescent material whose quenching due to Dexter energy transfer is inhibited. A high-luminance and high-reliability tandem OLED employing both technologies was achieved.

Author Keywords

OLED; blue phosphorescence; phosphor-sensitized fluorescence; spontaneous orientation polarization (SOP); giant surface potential (GSP)

1. Introduction

Organic light-emitting diode (OLED) displays are now widely used in smartphones and televisions, and an expansion of the market for wearable devices, such as augmented reality/virtual reality (AR/VR) devices, is anticipated [1,2]. High luminance and reliability are desired for OLED devices to meet the requirements of the high-luminance driving of AR/VR devices. Thus, reduced power consumption has also become vital. Commercially available OLED displays use highly efficient phosphorescent materials for green and red OLEDs. A fluorescent material is used for a blue OLED because a thermally activated delayed fluorescent (TADF) material and a phosphorescent material are unstable. This is because blue emission has the highest excitation energy among the three primary colors of light and is chemically unstable. Thus, an improvement in the reliability of blue OLEDs is required.

As highly efficient blue OLEDs, a phosphorescent OLED (PhOLED) using a platinum complex and a device using a multi-resonance (MR) TADF material have been reported [3,4]. Although such materials can emit light with high efficiency, each of them has a light emission mechanism that utilizes a triplet exciton with a long excitation lifetime. Thus, various kinds of two-molecule interactions, such as triplet–triplet annihilation and triplet–polaron quenching, are likely to be induced. Such intermolecular interactions successively generate high-energy excitons and polarons that cause the decomposition of organic materials, leading to device instability.

Thus, we developed a highly reliable blue phosphorescent device by combining two approaches, i.e., controlling a recombination region in a light-emitting layer (EmL) and shortening the excitation lifetime of triplet excitons via energy transfer between excitons. Specifically, electron injection into the EmL of the blue phosphorescent OLED was controlled by adjusting the spontaneous orientation polarization (SOP) in an electron-transport material (ETM) film. To shorten the excitation lifetime of a triplet exciton, a blue phosphor-sensitized fluorescent (PSF) OLED including a fluorescent material in which quenching due to Dexter energy transfer (DET) is inhibited was developed. A tandem OLED employing both aforementioned technologies exhibited high luminance and reliability.

2. Highly reliable blue phosphorescent OLED utilizing electron-transport layer with high SOP

An organic amorphous thin film formed by vacuum evaporation has been reported to exhibit molecular orientation, and molecular orientation is an important parameter that affects OLED characteristics, such as outcoupling efficiency and charge transport [5]. A recent study reported that the polarization charge derived from an orientation polarization of polar molecules in the evaporated film affects the charge-injection property of an OLED [6]. For an organic molecule with a permanent dipole moment (PDM) and an anisotropic molecular structure, SOP occurs in the evaporated film. When SOP occurs, a giant surface potential is generated in the film surface according to the PDM of the organic material. Considering that several kinds of evaporated films are stacked in an OLED, the polarization charge generated at an interface between the stacked films exhibiting different SOPs affects the carrier-injection properties between the layers. Therefore, the carrier-injection property of a device can be controlled when the SOP of each layer in the OLED is controlled.

Thus, we fabricated blue PhOLED devices in which ETM films with different SOPs were used as electron-transport layers (ETLs) and examined the device characteristics when the recombination regions were changed. Figure 1 shows the device structure and the SOPs of the material films. The SOPs of the films can be estimated by fabricating a device in which a film using the material and a film with a known SOP are stacked and subjecting the device to capacitance–voltage (C–V) measurements. For example, an Alq_3 film is known to exhibit an SOP of 48 mV/nm [7]. A comparison between the SOPs of the films fabricated using materials other than ET-01 and ET-02 used as ETMs shows that the films of two host materials (Host-01 and Host-02), which are EmL materials, exhibited high SOPs. Accordingly, the SOP generated in the EmL exceeded that in the layers. A negative polarization charge was generated at an interface of the EmL on the anode side and a positive polarization charge was generated at an interface of the EmL on the cathode side. The polarization charge lowers the initiation voltage for carrier injection into the EmL, and both carriers of holes and electrons injected from electrodes are rapidly injected into both EmL interfaces upon voltage application and then transported and recombined.

The influence of the SOPs of films using ET-01 and ET-02 in the ETLs of Devices 1 and 2 on carrier injection into the EmL is described below. The SOPs of the ET-01 and ET-02 films were 1.5 and 92.1 mV/nm, respectively. Considering that the ET-01 SOP was hardly observed, an interface between the ET-01 film and an adjacent hole-blocking layer (HBL) had a positive

ISSN 0097-996X/25/5601-0254-$1.00 © 2025

interface charge generated by the SOP of the HBL. The positive interface charge facilitated electron injection from the ETL to the HBL and EmL (Figure 2(a)). Conversely, since the SOP of the ET-02 film was high and the adjacent HB-01 film had a low SOP of 10.2 mV/nm, the interface between the ETL and HBL had a negative interface charge. This negative interface charge acted as an injection barrier; thus, electron injection from the ETL to the HBL was inhibited (Figure 2(b)). Electron injection to the EmL was more inhibited in Device 2 than in Device 1. In Device 2, ET-02 was doped with Liq to adjust electron mobility; however, this did not change the relationship between the SOPs of the HBL and ETL.

Table 1 lists the initial characteristics of the devices at 1000 cd/m^2. The driving voltage of Device 2 using ET-02 exceeded that of Device 1 using ET-01 with a low SOP. Owing to the occurrence of SOP in ET-02, a large amount of interface charge was generated at both ETL interfaces. Therefore, electron injection was more inhibited in Device 2 than in Device 1. At 1000 cd/m^2, the external quantum efficiencies (EQEs) of Devices 1 and 2 were 17.4% and 18.7%, respectively. Thus, a device with a favorable carrier balance was obtained using the ETL with inhibited electron injection.

Figure 3 shows the results of the devices driven at a constant current density of 10 mA/cm^2. LT90 indicates the time it takes for the luminance to decay by 10%. For Device 1, LT90 was 50 h, whereas that for Device 2 using the new ETL was 87 h, indicating that the LT90 for Device 2 was 1.7 times that for Device 1. Although both devices included the same EmL type, a major difference was observed in the driving reliability only because they contained different ETLs. This reflects the difference in the

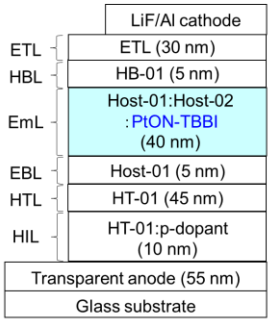

	ETL	Note
Device 1	ET-01	Low SOP ETL
Device 2	ET-02:Liq	High SOP ETL

Material	SOP (mV/nm)
ET-01	1.5
ET-02	92.1
HB-01	10.2
Host-01	34.7
Host-02	22.4
HT-01	17.3

Figure 1. Structures of Devices 1 and 2 and SOP of films.

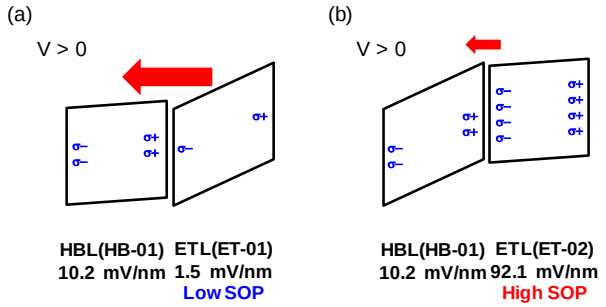

Figure 2. Diagrams of polarization charge and energy of stacked films. (a) ET-01 (b) ET-02.

Table 1. Characteristics of Devices 1 and 2 at 1000 cd/m^2.

Device	Voltage (V)	Current density (mA/cm^2)	CIE (x, y)	CE (cd/A)	EQE* (%)
1	4.80	3.26	(0.166, 0.282)	33.1	17.4
2	5.20	2.68	(0.164, 0.277)	35.1	18.7

* Lambertian assumption

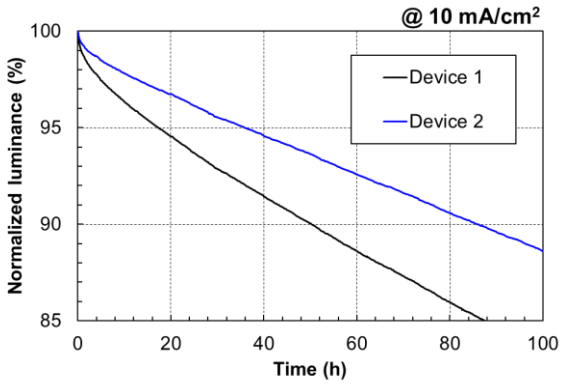

Figure 3. Driving test results of Devices 1 and 2.

electron-injection properties of the devices. In Device 2, electron injection was inhibited and the recombination region was expanded in the cathode direction, resulting in the delocalization of exciton distribution, which inhibits EmL degradation. Furthermore, the number of electrons injected into the EmL had possibly been reduced, leading to the inhibited degradation by exciton–polaron quenching. Thus, SOP control in the carrier-transport layer effectively improved the performance of the blue PhOLED.

3. Application to blue phosphor-sensitized fluorescent OLED

As a blue OLED with high efficiency and reliability, a PSF OLED with a phosphorescent material has been proposed as a sensitizer [8]. A phosphor-sensitized TADF OLED device, exhibiting high emission efficiency and color purity, using an MR TADF material as a fluorescent material has been reported [9]. However, the blue TADF material exhibits high triplet excitation energy and a long excitation lifetime because of the influence of a slow reverse intersystem rate constant. Thus, it is difficult to improve the inherent device stability. Consequently, the driving reliability is yet to reach a practical level.

Alternatively, a fluorescent material can be used as the emitter in the PSF OLED [8,10]. The fluorescent material undergoes a light emission process from a singlet excited state with a short excitation lifetime. Thus, it is advantageous in terms of its driving reliability over a phosphorescent material and a TADF material that pass through triplet excited states with long excitation lifetimes. In the PSF OLED, all excitons are trapped at the lowest triplet excited level (T1) that is radiative by intersystem crossing, and energy is transferred to the fluorescent material via Förster Resonance Energy Transfer (FRET). Although the device efficiency does not decline if the energy-transfer process is faultless, there is a conflicting process, i.e., DET, which impedes energy transfer. DET from the triplet excited state of the energy donor to the triplet excited state of the fluorescent material leads to thermal deactivation in the fluorescent material. Thus, the inhibition of this process is essential to maintain efficiency (Figure 4). To overcome this, we previously reported a PSF OLED using a fluorescent material that inhibits quenching due to DET [11]. Building on this concept, we discovered a blue fluorescent material, BFD-02, and used it for a PSF OLED.

We fabricated PSF OLED devices using a phosphorescent material as an energy donor and compared them with a PhOLED device. Figure 5 shows the device structures. A mixed layer of ET-02 and Liq was used as the ETL. Device 3 is a PhOLED without a fluorescent material. PtON-TBBI was used as a

phosphorescent material. The PhOLEDs in Devices 4 and 5, which were PSF OLEDs, were doped with BFD-01 and BFD-02, respectively, at a concentration of 1.5 wt%, and PtON-TBBI acted as an energy donor. BFD-01 is a conventional fluorescent material and BFD-02 is a fluorescent material with a molecular design in which DET from an energy donor is inhibited. The formation of BFD-02 was based on the molecular structure of BFD-01. Although FRET and DET are dependent on the intermolecular distance between an energy donor and acceptor, the intermolecular distance determines the predominance between FRET and DET. Considering that DET occurs within a short intermolecular distance compared with FRET, a molecular design for inhibiting DET was applied to BFD-02.

Figure 6 shows the electroluminescence (EL) spectra of the devices. Device 3 exhibited blue emission derived from PtON-TBBI with the Commission Internationale de L'éclairage (CIE) (x, y) chromaticity coordinates (0.144, 0.213). Similarly, Devices 4 and 5 exhibited blue emission derived from fluorescent materials with the CIE (x, y) chromaticity coordinates (0.139, 0.223) and (0.131, 0.241), respectively.

Figure 7 shows the EQE vs. luminance characteristics of the devices. The EQE of Device 3 at 1000 cd/m^2 was 22%, and that

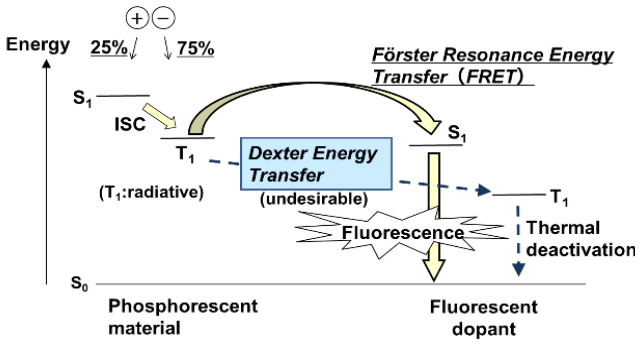

Figure 4. PSF OLED mechanism.

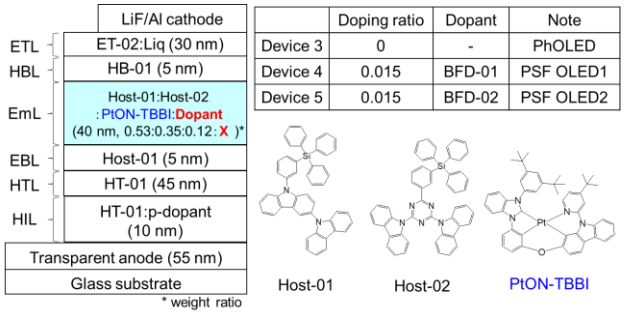

	Doping ratio	Dopant	Note
Device 3	0	-	PhOLED
Device 4	0.015	BFD-01	PSF OLED1
Device 5	0.015	BFD-02	PSF OLED2

Figure 5. Structures of Devices 3–5.

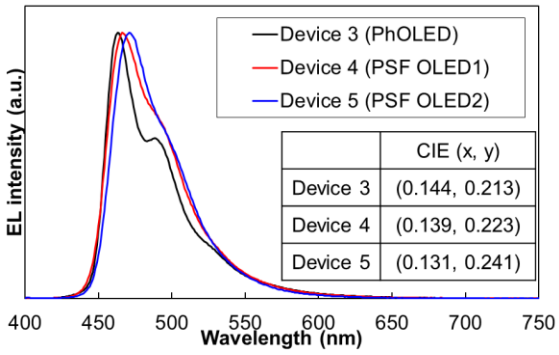

	CIE (x, y)
Device 3	(0.144, 0.213)
Device 4	(0.139, 0.223)
Device 5	(0.131, 0.241)

Figure 6. EL spectra of Devices 3–5.

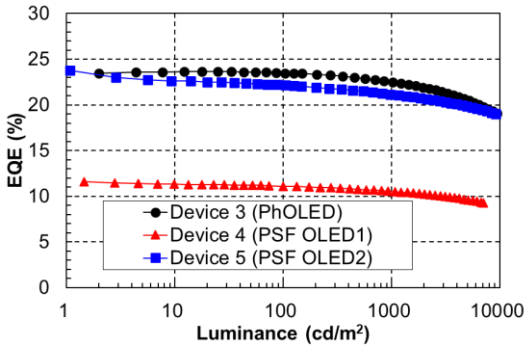

Figure 7. EQE characteristics of Devices 3–5.

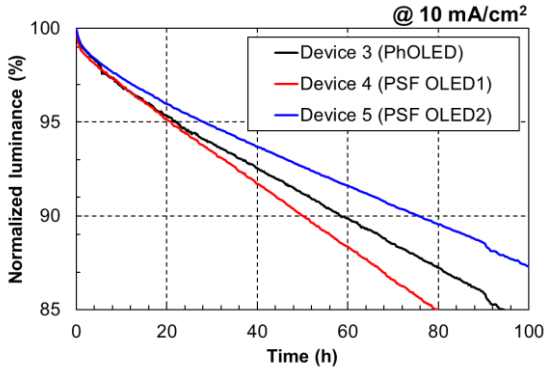

Figure 8. Driving test results of Devices 3–5.

of Device 4 containing BFD-01 was 11%. This was because of the influence of quenching due to DET, suggesting that an undesirable energy-transfer process occurred even when BFD-01 was added at a concentration of only 1.5 wt%. Contrarily, the EQE of Device 5 containing BFD-02 in which the doping concentration of the fluorescent material was the same as that in Device 4 was 21%, approximately that of Device 3. Thus, BFD-02 inhibited DET, compared with BFD-01, and achieved high efficiency while exhibiting the same emission color as PtON-TBBI, which served as an energy donor. The transient EL measurement of each device showed that the radiative decay time of Device 5 was 0.42 μs, which was shorter than that of Device 3 (0.94 μs). This was due to the addition of BFD-02, which shortened the excitation lifetime, increasing the reliability of the device.

Figure 8 shows the driving test results of the devices driven at a current density of 10 mA/cm^2. The reliability of Device 4 containing BFD-01 was lower than that of Device 3 (PhOLED) and exhibited decreased efficiency. Device 5 containing BFD-02 exhibited higher reliability with an EQE equivalent to that of Device 3 (PhOLED). The use of BFD-02, which inhibits quenching due to DET for the PSF OLED, increases the reliability of the device without quenching the excitation energy of the phosphorescent material functioning as the energy donor.

4. Application to tandem OLED

Assuming application to an actual display, a top-emission blue PSF tandem OLED (Device 6) with the proposed technologies was fabricated. A mixed layer of ET-03 and Liq was used for the ETL, and the ET-03 film had a high SOP of 44.3 mV/nm. The refractive index of the ET-03 film at a wavelength of 460 nm was 1.66, lower than that of the ET-01 film (1.90). This improved the outcoupling efficiency of the OLED, contributing to the overall efficiency [12]. Table 2 lists the device characteristics at 1000

cd/m^2. Figure 9 shows the driving reliability test results assuming white emission (D65) at 2500 cd/m^2 from a micro OLED display, whose specifications are shown in Table 3. We have developed c-axis-aligned crystalline oxide semiconductor (CAAC-OS) field-effect transistors (FETs) and low-temperature polysilicon and oxide (LTPO) FETs that are suitable for the backplane of the OLED display [13]. The backplane of the micro OLED display has a structure of monolithically stacking miniaturized CAAC-OS FETs over complementary metal-oxide-semiconductor (CMOS) large scale integration (LSI) on a Si substrate. To achieve the red, green, and blue (RGB) side-by-side micro OLED display with a high resolution and aperture ratio, it is optimal to perform photolithography, which is a patterning technique for OLEDs, developed by our company [14]. In the blue OLED developed in this study, LT95, which indicates the time it takes for the luminance to attenuate by 5% from the initial driving stage, is 230 h. The LT95 for the blue PSF tandem OLED was 3.2 times that for a conventional blue phosphorescent tandem OLED under the same driving conditions. Accordingly, a display, in which the LT95 for each RGB pixel exceeds 200 h, can be fabricated. Using our highly efficient blue tandem OLED, the current amount of blue pixels can be reduced by half compared with the case of a conventional blue fluorescent tandem OLED. The results demonstrate that a highly efficient blue OLED with high luminance, low power consumption, and high reliability was obtained.

Table 2. Characteristics of Device 6.

Device	Voltage (V)	Current density (mA/cm^2)	CIE (x, y)	CE (cd/A)	EQE* (%)
6	12.4	3.53	(0.124, 0.0911)	29.3	39.2

* Lambertian assumption

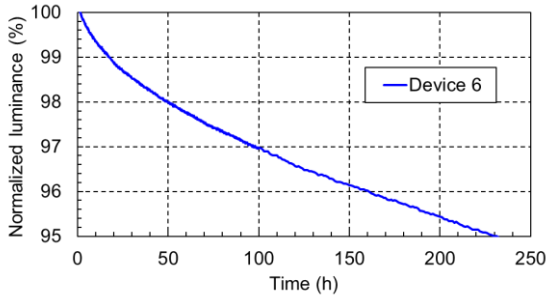

Figure 9. Driving test result of Device 6.

Table 3. Panel specifications

Screen diagonal	1.50 inches
Structure	OS LSI / Si LSI
Resolution	3840 × 2880
Pixel size	7.92 μm × 7.92 μm
Pixel density	3207 ppi
Aperture ratio	54.0%
Pixel arrangement	S-stripe
Coloring method	RGB side-by-side
Emission type	Top emission
Source driver	Integrated
Scan driver	Integrated
Luminance	2500 cd/m^2
Color gamut	DCI-P3 95.0%

5. Conclusions

A highly reliable blue PhOLED was developed by adjusting the SOP of an ETL. A high SOP causes a large amount of negative polarization charge at the interface between the ETL and an HBL, such that the electron-injection property of the device can be inhibited. In device design that considers the recombination region, exciton density, and polaron density of the blue PhOLED, the SOP can be a useful indicator of material selection. A fluorescent material that inhibits quenching due to DET was used for the blue PSF OLED to achieve high reliability while maintaining an efficiency equivalent to that of the PhOLED. By applying these techniques to the tandem OLED, we successfully developed a blue OLED with high luminance and reliability.

6. References

[1] S. Yamazaki et al., US patent, 8,344,363 B2

[2] J. Xiong et al., "Augmented reality and virtual reality displays: emerging technologies and future perspectives", Light.: Sci. Appl., 10, 216 (2021).

[3] J. Sun, et al., "Exceptionally stable blue phosphorescent organic light-emitting diodes", Nat. Photonics, 16, pp. 212-218 (2022).

[4] T. Hatakeyama et al., "Ultrapure Blue Thermally Activated Delayed Fluorescence Molecules: Efficient HOMO–LUMO Separation by the Multiple Resonance Effect", Adv. Mat., 28, pp. 2777-2781 (2016).

[5] D. Yokoyama et al., "Molecular orientation in small-molecule organic light-emitting diodes", J. Mater. Chem., 21, pp. 19187-19202 (2011).

[6] Y. Noguchi et al., "Spontaneous orientation polarization in organic light-emitting diodes", Jpn. J. Appl. Phys., 58, SF0801 (2019).

[7] E. Ito et al., " Spontaneous buildup of giant surface potential by vacuum deposition of and its removal by visible light irradiation", J. Appl. Phys., 92, pp. 7306-7310 (2002).

[8] S. Nam et al., "Improved Efficiency and Lifetime of Deep-Blue Hyperfluorescent Organic Light-Emitting Diode using Pt(II) Complex as Phosphorescent Sensitizer", Adv. Sci, 8, 2100586 (2021).

[9] E. Kim et al., "Highly efficient and stable deep-blue organic light-emitting diode using phosphor-sensitized thermally activated delayed fluorescence", Sci. Adv., 8, eabq1641 (2022).

[10] H.-G. Kim et al., "Highly Efficient, Conventional, Fluorescent Organic Light-Emitting Diodes with Extended Lifetime", Adv. Opt. Mater., 5, 1600749 (2017).

[11] S. Seo et al., "Fluorescent OLED Achieving External Quantum Efficiency over 20% and Longer Lifetime than Phosphorescent OLED", SID Sym., Dig. Tech. Pap., 50, pp. 42-45. (2019)

[12] T. Watabe et al., "Extremely High-Efficient OLED Achieving External Quantum Efficiency over 40% by Carrier Injection Layer with Super-Low Refractive Index", SID Symp. Dig. Tech. Pap., pp. 332-335. (2018).

[13] S. Yamazaki, K. Takahasi., JP patent, 7,554,334S.

[14] S. Fukuzaki et al., "High-luminance and Highly Reliable Tandem OLED Display Including New Intermediate Connector Designed for Photolithography Applications", Journal of SID.2024;32:309-319 (2024).